Available online at www.sciencedirect.com

ScienceDirect

Ceramics International 40 (2014) 2267–2274

CERAMICS INTERNATIONAL

www.elsevier.com/locate/ceramint

Nanocrystalline indium-based oxides by tartarate precursor route

Dana Gingasu, Ioana Mindru*, Luminita Patron, Gabriela Marinescu, Silviu Preda, Jose Maria Calderon-Moreno, Nicolae Stanica, Cristian Andronescu

Ilie Murgulescu Institute of Physical Chemistry of the Romanian Academy, Splaiul Independentei 202, Bucharest 060021, Romania

Received 1 July 2013; received in revised form 30 July 2013; accepted 30 July 2013
Available online 7 August 2013

Abstract

$Cu_2In_2O_5$ with orthorhombic structure and $CdIn_2O_4$ spinel oxide have been synthesized by the precursor method *via* the tartarate route. The complex precursors, $(NH_4)_{12}[Cu_2In_2(C_4O_6H_4)_2(C_4O_6H_3)_6]\cdot 6H_2O$(**I**) and $(NH_4)_4[CdIn_2(C_4O_6H_4)_4(OH)_4(H_2O)_2]$ (**II**), have been characterized by infrared spectroscopy (IR), ultraviolet–visible spectroscopy (UV–Vis), luminescence spectroscopy, magnetic measurements and thermal analysis. Indium-based oxides have been investigated and characterized by X-ray diffraction (XRD), scanning electron microscopy (SEM), UV–vis spectroscopy and magnetic measurements. Both indates are nanocrystalline powders. The average crystallite size is around 40–60 nm.

Keywords: A. Powders: chemical preparation; B. Spectroscopy; $Cu_2In_2O_5$; $CdIn_2O_4$

1. Introduction

Transparent conducting oxides (TCOs) are materials of both fundamental interest and technological importance. In the last decade, *n* - type TCOs with different structures have been used in photovoltaic cells, transparent electronic devices and other optical displays due to their improved optical, electrical, thermal and magnetic properties [1–4]. Transparent conducting oxides like: $MgIn_2O_4$ [1,2,5], $CdIn_2O_4$ [6,7], $ZnGa_2O_4$ [8], $CdGa_2O_4$ [9], $Zn_kIn_2O_{3+k}$ [10] and $Cu_2In_2O_5$ [11] have been studied. At the same time, $CdIn_2O_4$ has been extensively investigated and used for gas detection due to of its sensitivity to different gaseous species like ethanol, acetone [4], formaldehyde [12], chlorine [13], hydrocarbons [14] and H_2S [15].

Synthesis routes have played a crucial role in obtaining these mixed oxides and influencing their properties. Transparent mixed oxides have been synthesized through various methods such as the conventional solid state method involving the mechanical mixing of metal oxides followed by calcination at high temperatures (>1000 °C) for long periods varying from 4 hours to 2 days [10,16,17], the co-precipitation method [18], the aqueous/nonaqueous sol–gel procedure [4,12,19,20] and the self-template reaction [21].

As far as we know, there are only few studies regarding the preparation of these oxides by the *precursor method* (also known as the complexation method) which consists in the thermal decomposition of multimetallic complex compounds [22].

The main goal of this research is the preparation of nanocrystalline $Cu_2In_2O_5$ and $CdIn_2O_4$ by the precursor method through the *tartarate precursor route*. The precursors are polynuclear tartarate multimetallic compounds. Both precursors and indium based oxides are characterized.

2. Experimental

2.1. Reagents

All chemicals: $Cu(NO_3)_2\cdot 3H_2O$, $InCl_3$, $Cd(NO_3)_3\cdot 4H_2O$, tartaric acid ($C_4O_6H_6$) are of reagent quality (Merck).

2.2. $Cu_2In_2O_5$ preparation from tartarate precursor (*I*)

To obtain the $Cu_2In_2O_5$ tartarate precursor, the following system was studied: copper(II) nitrate–indium(III) chloride-tartaric acid. $Cu(NO_3)_2\cdot 3H_2O$ and $InCl_3$ were dissolved in minimum amount of

*Corresponding author. Tel.: +40 021 3167912; fax: +40 021 3121147.
E-mail address: imandru@yahoo.com (I. Mindru).

0272-8842/$ - see front matter © 2013 Elsevier Ltd and Techna Group S.r.l. All rights reserved.
http://dx.doi.org/10.1016/j.ceramint.2013.07.146

distilled water and mixed with an aqueous solution of tartarate acid in a 2:2:8 M ratio under continuous stirring. Ethanol was added to the final solution until a blue precipitate was formed. The pH was raised to 6 by adding NH_4OH:ethanol (1:1). After 24 h at 4 °C, the precipitate was filtered and dried over P_4O_{10}.

Elemental analysis was consistent with the formula:

$(NH_4)_{12}[Cu_2In_2(C_4O_6H_4)_2(C_4O_6H_3)_6]\cdot 6H_2O$ **(I)**: Anal.: Calcd.: In%: 12.35; Cu%: 6.93; C%: 20.66; N%: 9.03; H%: 4.62; found: In%: 12.65; Cu%: 7.21; C%: 20.39; N%: 8.43; H%: 5.3.

In order to prepare well-crystallized $Cu_2In_2O_5$, this compound was calcined for 12 h at 950 °C.

2.3. $CdIn_2O_4$ preparation from tartarate precursor (*II*)

The $CdIn_2O_4$ tartarate precursor was obtained from the system: cadmium(II) nitrate–indium(III) chloride-tartaric acid. $Cd(NO_3)_3\cdot 4H_2O$ and $InCl_3$ were dissolved in minimum amount of distilled water. An aqueous solution of tartaric acid was then added such that the molar ratio of metal ions and tartaric acid was 1:2:4. A white precipitate was formed by adding ethanol. A solution of NH_4OH:C_2H_5OH (1:1) was added until the pH rose to ~6. After 24 h at 4 °C, the white compound was filtered, washed with ethanol and dried over P_4O_{10}.

Elemental analysis was consistent with the formula:

$(NH_4)_4[CdIn_2(C_4O_6H_4)_4(OH)_4(H_2O)_2]$ **(II)**: Anal.: Calcd.: In%: 20.68; Cd%: 10.12; C%: 18.22; N%: 4.68; H%: 3.42; found: In%: 20.40; Cd%: 9.89; C%: 17.99; N%: 5.04; H%: 3.60.

Calcination of this precursor, $(NH_4)_4[CdIn_2(C_4O_6H_4)_4(OH)_4(H_2O)_2]$ **(II)**, at 900 °C for 10 h resulted in the formation of well-crystallized $CdIn_2O_4$.

2.4. Characterization techniques

The metal content of the complex compounds was determined by atomic absorption spectroscopy with an SAA1 instrument and by gravimetric techniques; the C, N and H values were obtained using a Carlo Erba Model 1108 CHNSO elemental analyzer.

The IR spectra of tartarate precursors and indates were recorded on KBr pellets with a JASCO FTIR 4100 spectrophotometer in the 4000–400 cm^{-1} range. Absorption spectra were made with a JASCO V-670 spectrophotometer.

The photoluminescence spectrum of the cadmium indium tartarate precursor was examined using a JASCO FP 6500 spectrofluorimeter.

The thermal measurements (TG, DTG and DTA) were performed using Mettler Toledo TGA-SDTA 851 equipment in an air static atmosphere. The measurements were carried out in the range of 25–1000 °C with 10 °C min^{-1} heating rate.

X-ray diffraction data were collected using parallel beam geometry on Rigaku's Ultima IV X-ray powder diffractometer, with Cu Kα radiation ($\lambda = 1.54$ Å), CBO optics, operating at 40 kV and 30 mA, 0.02 ° step size and 5 °/min scan speed. Phase identification and Rietveld analysis were performed using Rigaku's PDXL software, with Whole Pattern Fitting (WPF) module, connected to ICDD PDF-2 database.

Scanning Electron Microscopy (SEM) was used to examine the surface morphology, using a Zeiss EVO LS10 environmental SEM at an operating voltage of 30 kV and a FEI 3D FEG SEM microscope, equipped with an energy dispersive X-ray spectroscopy (EDS) detector.

The magnetic measurements of both copper–indium tartarate complex compound and copper–indium oxide were performed with VSM Lake Shore equipment.

3. Results and discussion

3.1. Characterization of the tartarate precursors

In(III) coordination compounds containing carboxylate anions as ligands have been well known for more than 30 years [23,24]. Numerous example of 1D, 2D, 3D indium carboxylate extended structures have been investigated [25–30].

Tartaric acid has been selected as building block for 1D, 2D, 3D frameworks due to the diversity of the binding modes of carboxyl and hydroxyl groups. A survey of the literature shows the main types of tartarate complex compounds [31–33].

The hydrothermal synthesis of indium tartarate polymer compounds $[In(L\text{-}TAR)\ H_2O]\cdot 0.5H_2O$ containing tartarate trianions (TAR) with a 2D structure and [In(OH)(D/L)–TAR]·$2H_2O$ with a 3D framework has been reported recently [34].

Jian and co.[35] obtained a novel two-dimensional coordinate polymer containing a porous framework: $\{[Cu_2(C_4H_4O_6)_2(H_2O)_2]\cdot 4H_2O\}_\infty$ using the reaction between fresh $Cu(OH)_2$ and tartaric acid in hydrothermal conditions.

Due to its multiple functions, the tartaric acid has also been used as ligand in the synthesis of heteropolynuclear coordination compounds [22,36–39].

Our aim was to synthesize two heteropolynuclear complex compounds containing In^{3+} and M^{2+} (where M^{2+}=Cu^{2+}, Cd^{2+}) as precursors for $Cu_2In_2O_5$ and $CdIn_2O_4$, respectively. The $(NH_4)_{12}[Cu_2In_2(C_4O_6\ H_4)_2(C_4O_6\ H_3)_6]\cdot 6H_2O$ **(I)** and $(NH_4)_4[CdIn_2(C_4O_6H_4)_4(OH)_4(H_2O)_2]$ **(II)** compounds have been investigated by IR, UV–vis, luminescence spectroscopy and magnetic measurements.

The IR spectra of the compounds **I** and **II** were recorded in the 400–4000 cm^{-1} range and were compared to those of tartaric acid and sodium tartarate, respectively. The IR spectrum of tartaric acid showed a band at 1740 cm^{-1} assigned to ν(CO) vibration. After the formation of coordination compounds, this band disappeared and was replaced in the IR spectra of these compounds by two intense bands ν_{asym}(OCO) (1594 cm^{-1} for **I** and 1600 cm^{-1} for **II**) and ν_{sym}(OCO) (1396 cm^{-1} for **I** and 1398 cm^{-1} for **II**) (Fig.1).

The magnitude of the separation $\Delta\nu = \nu_{asym} - \nu_{sym}$ is a spectroscopic criterion indicative of the coordination mode of carboxylate anions. The $\Delta\nu$ values in the range 190–210 cm^{-1} observed in these spectra are smaller than the $\Delta\nu$ value of the ionic compound ($\Delta\nu(Na_2L) = 240\ cm^{-1}$) and suggest a bidentate coordination for the carboxylate groups of tartarate anions.

At the same time, the analysis of the spectra within the 1000–1150 cm^{-1} range reveals a difference between the spectrum of the free acid and the spectra of the tartarate

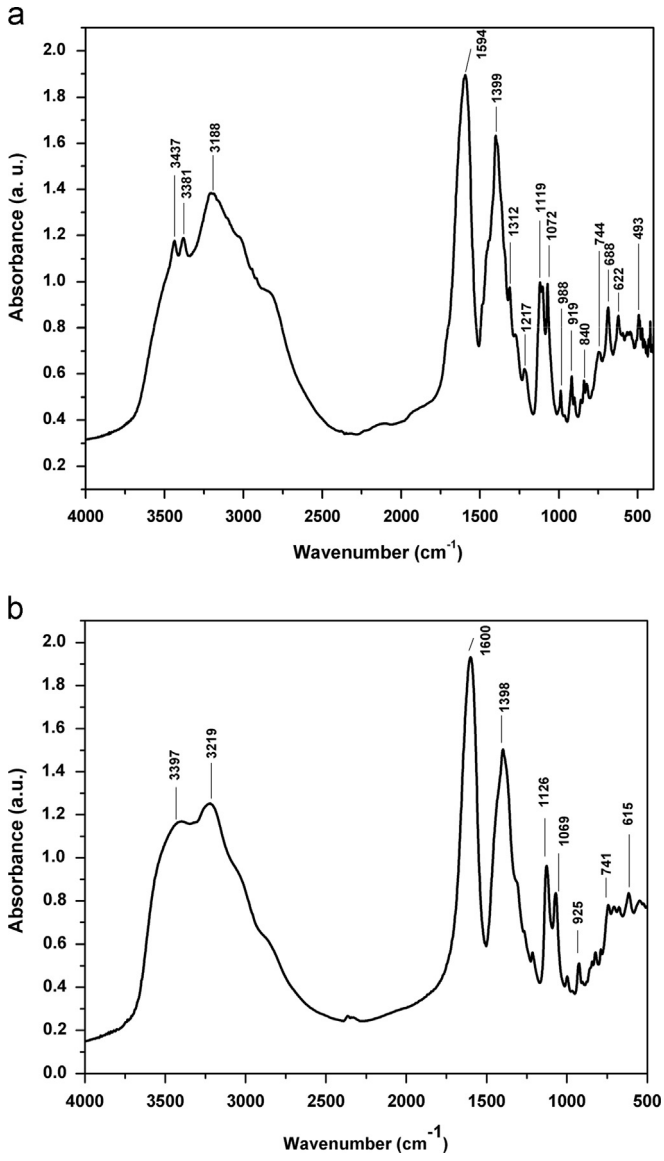

Fig. 1. IR spectra of (a) $(NH_4)_{12}[Cu_2In_2(C_4O_6H_4)_2(C_4O_6H_3)_6]\cdot 6H_2O$, (b) $(NH_4)_4[CdIn_2(C_4O_6H_4)_4(OH)_4(H_2O)_2]$.

compounds: the peak assigned to the C–O stretching vibration of the secondary OH groups appearing in the spectrum of the free acid (1100–1130 cm^{-1}) is splitted in two components in the IR spectra of the tartarate compounds (1060–1130 cm^{-1}). The splitting can be explained by a dissimilar bonding of the secondary OH groups to two different metal ions.

Both tartarate compounds exhibit a broad and intense band in the range 2800–3400 cm^{-1}. This band can be assigned to the vibration of water molecules or/and the formation of hydrogen bonds between water and/or hydroxyl groups. The presence on this band of a distinct shoulder at ~3200 cm^{-1} can be assigned to $\nu_3(NH_4^+)$ stretching vibration. The band can be correlated with another one between 1390 and 1480 cm^{-1} due to $\nu_4(NH_4^+)$ deformation, this band being however overlapped by the $\nu_{sym}(OCO)$ [40].

The absorption spectrum of the compound **I** is presented in Fig. 2. The band located at ~252 nm is most probably the

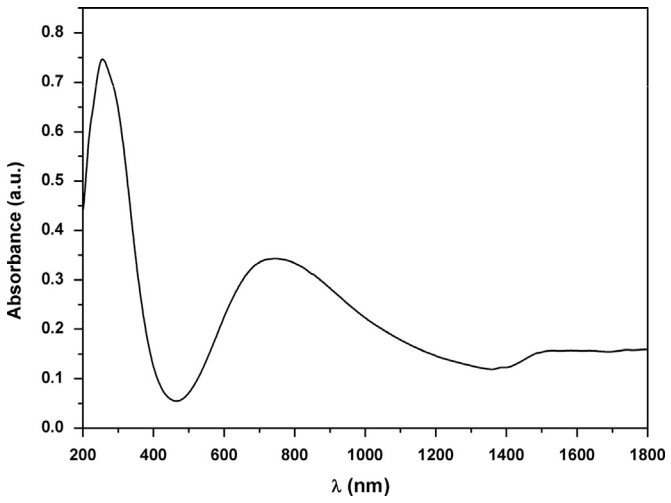

Fig. 2. Absorption spectrum of $(NH_4)_{12}[Cu_2In_2(C_4O_6H_4)_2(C_4O_6H_3)_6]\cdot 6H_2O$.

ligand's own band. The broad band appearing in the range 700–1100 nm can be attributed to d–d transitions characteristic of copper(II) (d^9) with distorted square pyramidal stereochemistry [41].

The $(NH_4)_{12}[Cu_2In_2(C_4O_6H_4)_2(C_4O_6H_3)_6]\cdot 6H_2O$ compound is paramagnetic. The value of the magnetic moment ~2.39 BM ($\chi_g exp = 0.8\times 10^{-6}$ emu/g at $T = 296$ K) is very close to the one calculated for a dinuclear Cu(II) compound ($\mu = 2.44$ BM). This behavior is consistent with the absence of interaction between these two Cu(II) ions.

The emission spectrum in solid state was measured for the compound **II** at room temperature. Excited with 320 nm, the compound exhibits a strong emission band centered at 409 nm (Fig. 3), while the free ligand shows an emission band at about 405 nm. The fluorescent emission of the compound originates from the ligand transitions.

The thermal behavior of these compounds was investigated to establish the decomposition steps and the optimal conditions for the conversion of tartarate compounds into $Cu_2In_2O_5$ and $CdIn_2O_4$, (Fig. 4).

The thermal decomposition of $(NH_4)_{12}[Cu_2In_2(C_4O_6H_4)_2(C_4O_6H_3)_6]\cdot 6H_2O$ (**I**) occurs in three steps (Fig. 4a). The weight loss (~5.18%) associated with an endothermic DTA peak below 150 °C corresponds to the loss of water molecules from the lattice (first step). The other two exothermic peaks on the DTA curve, accompanied by a very large weight loss (~70.69%) on the TG curve, are caused by the decomposition of tartarate ligands. This decomposition taking place in consecutive and/or overlapping steps (better observed on the DTG curve) is a pyrolytic process. It is accompanied by the evolution of large amount of gases (such as CO, CO_2, water and vapor). Thermal analysis of the precursor showed that the decomposition is complete at a temperature below 550 °C.

The thermal decomposition of $(NH_4)_4[CdIn_2(C_4O_6H_4)_4(OH)_4(H_2O)_2]$ (**II**), (Fig. 4b) occurs in four steps. The weight loss (~11.4%) associated with an endothermic DTA peak in the temperature range 25–200 °C corresponds to the loss of four water molecules and four ammonia molecules. The next two steps on the TG curve, between 200 °C and 470 °C,

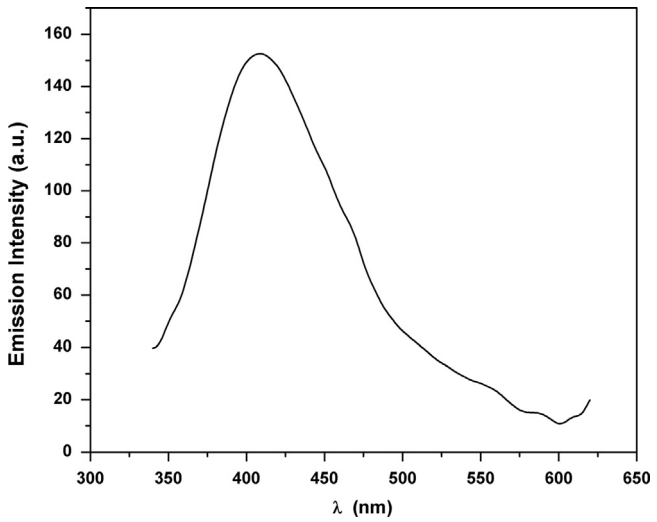

Fig. 3. Solid-state emission spectrum of $(NH_4)_4[CdIn_2(C_4O_6H_4)_4(OH)_4(H_2O)_2]$.

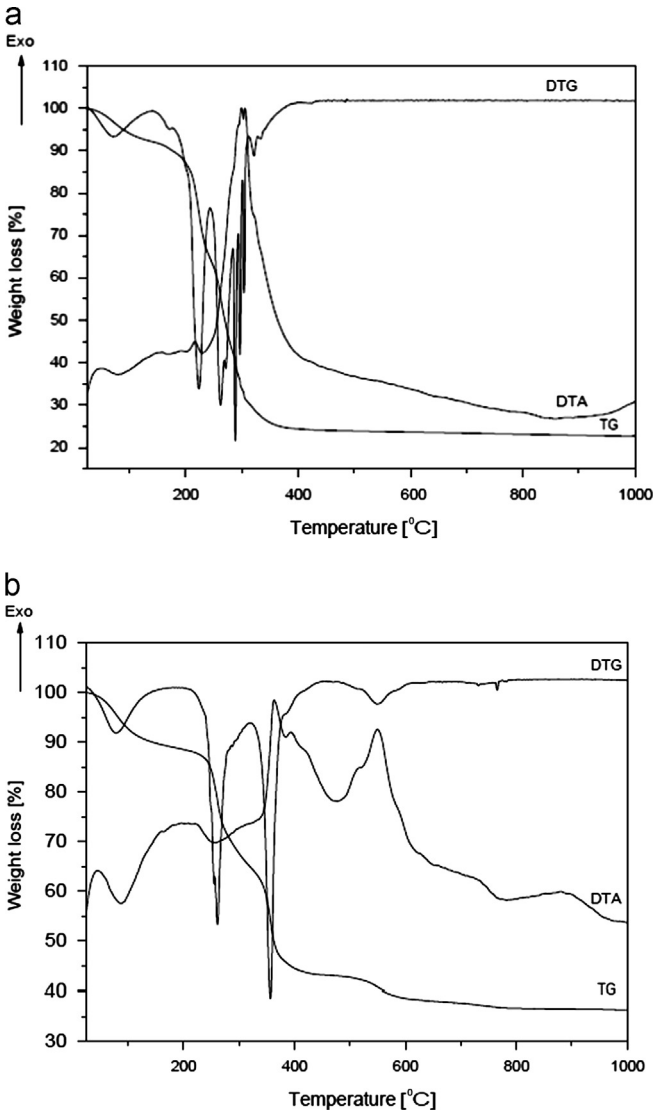

Fig. 4. TG, DTG and DTA curves of (a) $(NH_4)_{12}[Cu_2In_2(C_4O_6H_4)_2(C_4O_6H_3)_6]\cdot 6H_2O$ and (b) $(NH_4)_4[CdIn_2(C_4O_6H_4)_4(OH)_4(H_2O)_2]$.

correspond to a weight loss ~45.16% and are caused by the decomposition of tartarate ligands. This process is accompanied by a sharp, strong exotermic process on the DTA curve. The last decomposition step on the TG curve, between 470 and 900 °C, accompanied by an exothermic peak on the DTA curve, corresponds most probably to the decomposition of an oxocarbonate intermediate, $CdIn_2O_2(CO_3)_2$ (weight loss ~6.52%). The IR spectrum of $CdIn_2O_2(CO_3)_2$ recorded in the 400–4000 cm^{-1} range exhibits bands assigned to vibrational frequencies of CO_3^{2-}: $\nu_1 \sim 1080\ cm^{-1}$, $\nu_3 \sim 1492\ cm^{-1}$ and $\nu_4 \sim 700\ cm^{-1}$. The thermal decomposition is complete at about 900 °C.

Thermal analysis showed that the decomposition of these tartarate precursors is quite different. For the first compound, the decomposition finished at a temperature below 550 °C, while for the second compound the process finished at around 900 °C. This is due to the difference in the composition of these compounds. The existence of more tartarate anions and NH_4^+ cations in compound **I** induces a pyrolitic combustion process similar to self-propagating combustion, leading to a significant decrease in the final temperature.

3.2. Characterization of $Cu_2In_2O_5$

It is well known that $Cu_2In_2O_5$ crystallizes in two phases: an orthorhombic crystal structure and a monoclinic one [42–44].

The final product obtained after the thermal decomposition of the complex compound $(NH_4)_{12}[Cu_2In_2(C_4O_6H_4)_2(C_4O_6H_3)_6]\cdot 6H_2O$ (**I**) was calcined at 950 °C for 12 h. The X-ray diffraction pattern confirmed the formation of ultrafine orthorhombic $Cu_2In_2O_5$ with space group $P2_1nb$ (33) (Fig. 5). The lattice constants are $a=12.297$, $b=10.536$ and $c=3.276$ Å (ICDD PDF 01-070-1082). The average crystallite size is found to be ~40 nm. Some reflections of In_2O_3 (ICDD PDF. 00-006-0416) and CuO (ICDD PDF 01-089-2529) were present as well.

SEM micrographs and the EDS spectrum of the $Cu_2In_2O_5$ powder prepared as described above are shown in Fig. 6. The particles observed in SEM are faceted, with uniform particle size (Fig. 6a, b). According to the crystalline size measured from XRD results, the faceted particles observed in SEM must be formed of several primary nanocrystallites. EDS measurements detected the presence of Cu, Cd and O in the oxide powder, quantitative analysis gave a Cu:In atomic ratio of 2:2 ($\pm$ 0.03) in all analyzed regions.

Magnetic susceptibility was measured in the temperature range 80–300 K (Fig. 7). The χ(T) curve in this temperature range follows the Curie–Weiss law $\chi = C/(T+\theta)$.

The experimental value of the effective magnetic moment, $\mu_{eff}=1.76$ BM, is in agreement with the theoretical value of 1.98 BM (derived for $S=1\backslash 2$, with $g=2.28$) [42,45,46] and confirms the existence of Cu^{2+} state in $Cu_2In_2O_5$.

The absorption spectrum of $Cu_2In_2O_5$ recorded in the 200–1800 nm, exhibits two bands around ~400 nm and ~700 nm which can be assigned to the transitions to the components of the ^2E level (in T_d) in D_{2d} symmetry (Fig. 8) [41].

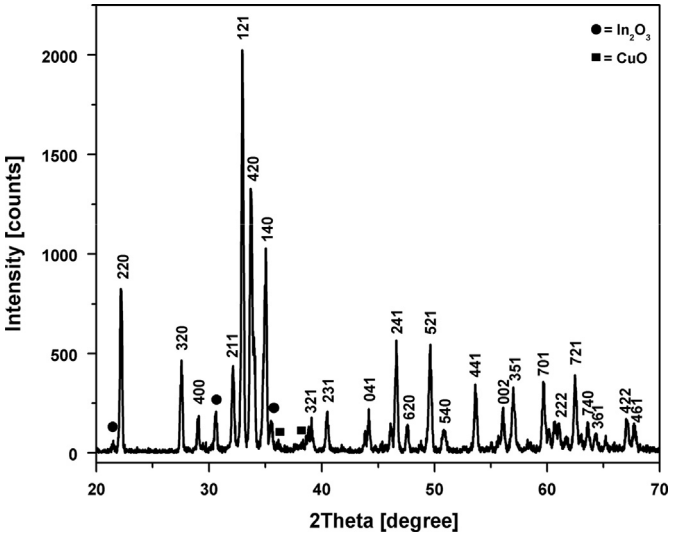

Fig. 5. XRD patterns of $Cu_2In_2O_5$.

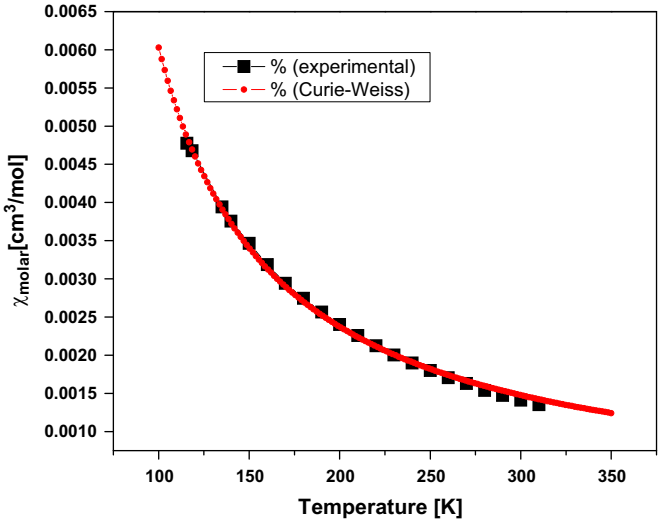

Fig. 7. Temperature dependence of magnetic susceptibility for $Cu_2In_2O_5$ at an applied magnetic field of 500 Oe.

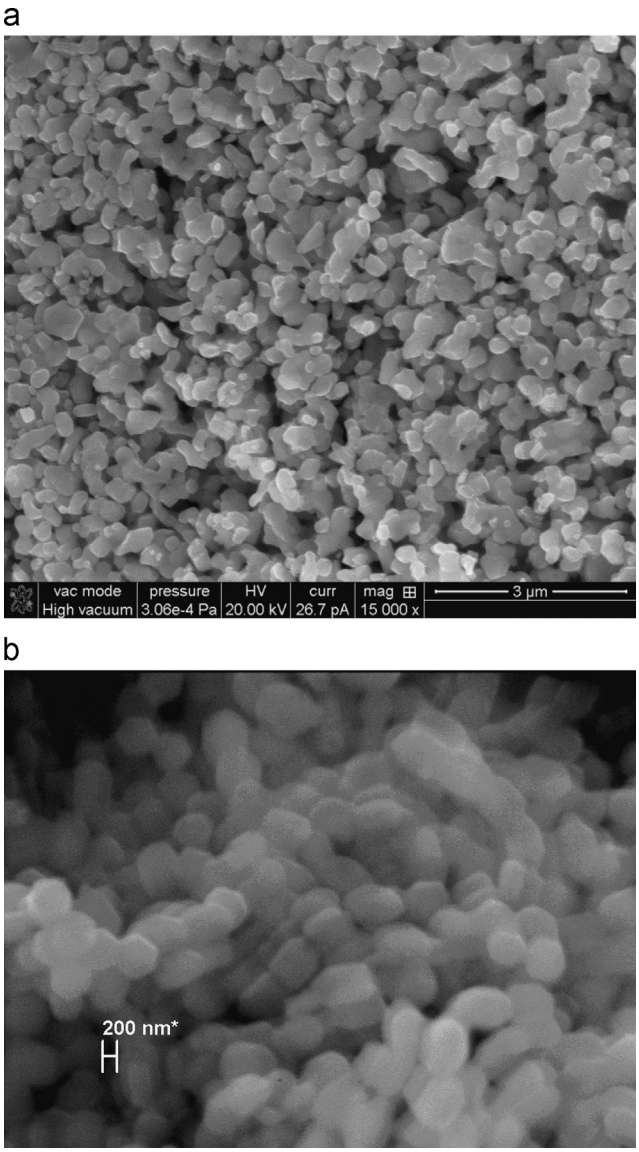

Fig. 6. (a, b) SEM micrographs of $Cu_2In_2O_5$ powder, at different magnifications.

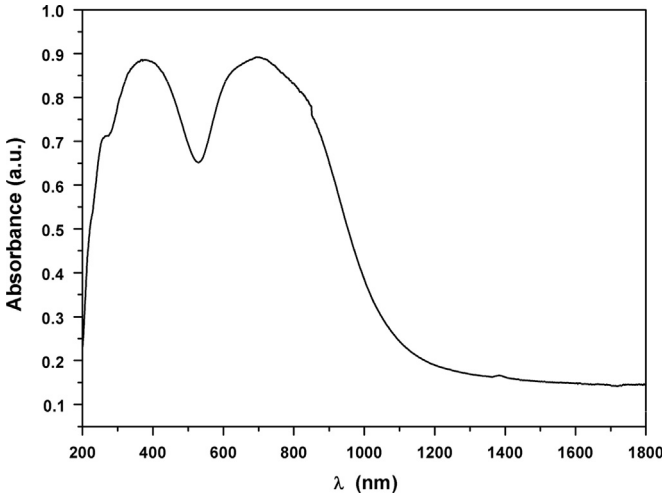

Fig. 8. Absorption spectrum of $Cu_2In_2O_5$.

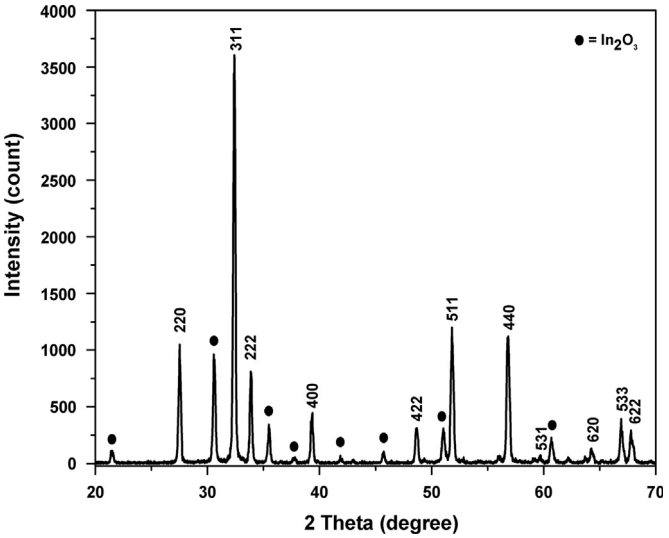

Fig. 9. XRD patterns of $CdIn_2O_4$.

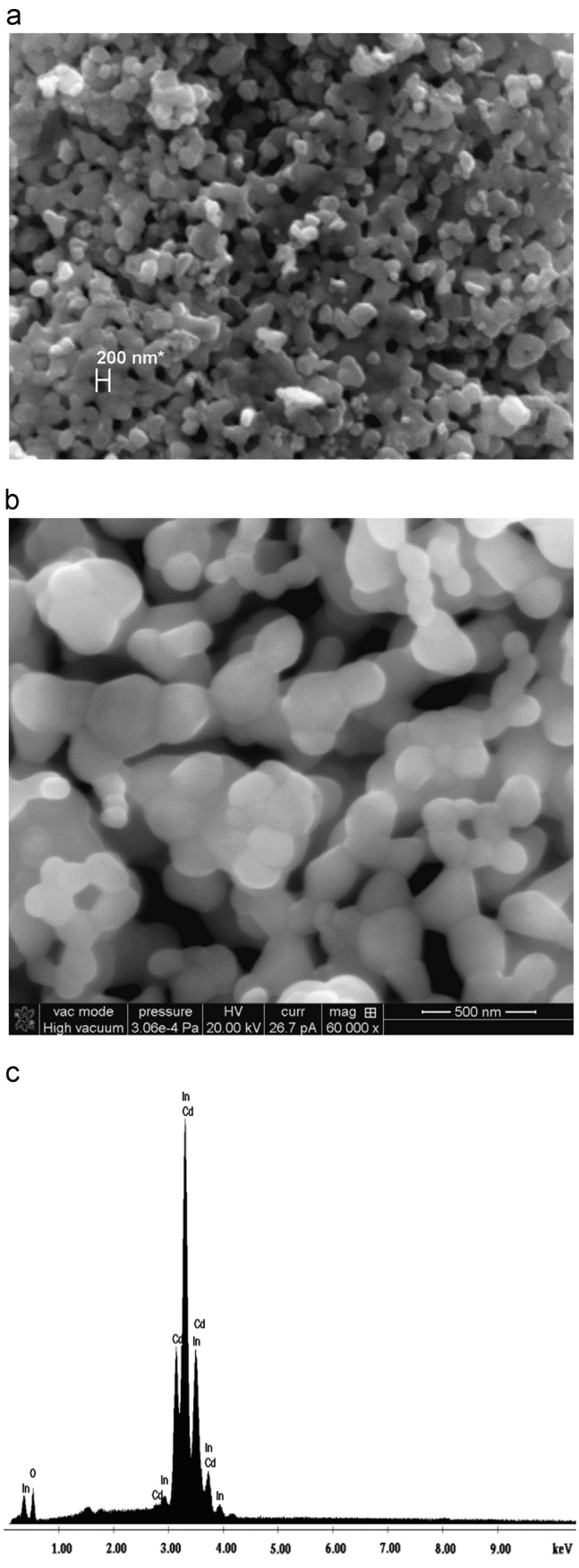

Fig. 10. (a, b) SEM micrographs and (c) EDS spectrum of oxide $CdIn_2O_4$ powder.

3.3. Characterization of $CdIn_2O_4$

The final compound was treated for 10 h at 900 °C to obtain the $CdIn_2O_4$ spinel oxide through the decomposition of the tartarate complex $(NH_4)_4[CdIn_2(C_4O_6H_4)_4(OH)_4(H_2O)_2]$ **(II)**. The phase composition was established by X-ray diffraction patterns (Fig. 9). The compound showed well-developed diffraction lines of the $CdIn_2O_4$ spinel phase (ICDD PDF 074–0841). The reflections were indexed to the $CdIn_2O_4$ space group *Fd3m* (227), $a=9.163$ Å. The average crystallite size was found to be ~60 nm. Some reflections of In_2O_3 were present as well.

The SEM micrograph of the $CdIn_2O_4$ powder is shown in Fig. 10. Uniform particles with size between 100 and 200 nm are observed (Fig. 10a, b). $CdIn_2O_4$ powders obtained by the hydrothermal route or the chemical coprecipitation method generally present the formation of large micron-sized agglomerated particles [12]. This phenomenon is not observed in our case. Compared to other methods, the precursor route results in a more uniform particle size and prevents the formation of large agglomerates. EDS measurements (Fig. 10c) detected the presence of Cd, In and O in the oxide powder, quantitative analysis gave a Cd:In atomic ratio of 1:2 (± 0.04) in all analyzed regions.

4. Conclusions

$Cu_2In_2O_5$ with orthorhombic structure and $CdIn_2O_4$ spinel oxide have been synthesized by the precursor method *via* the tartarate route. Heating treatment at 950 °C/12 h and 900 °C/10 h was required to obtain well crystallized $Cu_2In_2O_5$ and $CdIn_2O_4$, respectively.

Indium-based oxides have been investigated and characterized by XRD, SEM, UV–vis spectroscopy and magnetic measurements. The average crystallite size was found to be 40–60 nm.

These results proved that it is possible to obtain nanoparticles indium-based oxides with varied structures by the precursor method *via* the tartarate route.

Acknowledgments

Support of the EU (ERDF) and Romanian Government under POS-CCE O 2.2.1 project INFRANANOCHEM-Nr. 19/01.03.2009, allowing the acquisition of the research infrastructure, is gratefully acknowledged. The work also benefits from the support of the "Materials Science and Advanced Characterization Methods" Programme of the "Ilie Murgulescu" Institute of Physical Chemistry financed by the Romanian Academy.

References

[1] A.M.E. Raj, G. Selvan, C. Ravidhas, M. Jahachandran, C. Sanjecviraja, Magnesium indium oxide ($MgIn_2O_4$) spinel thin films: chemical spray pyrolysis(CSP) growth and materials characterizations, Journal of Colloid and Interface Science 328 (2008) 396–401.

[2] A.M.E. Raj, V. Senthilkumar, V. Swaminathan, J. Wollschlager, M. Suendorf, M. Neumann, M. Jayachandran, C. Sanjuviraja, Studies

on transparent spinel magnesium indium oxide thin films prepared by chemical spray pyrolysis, Thin Solid Films 517 (2008) 510–516.
[3] A.M.E. Raj, C. Ravidhas, R. Ravishankar, A.R. Kumar, G. Selvan, M. Jahachandran, C. Sanjecviraja, Optimized deposition and characterization of nanocrystalline magnesium indium oxide thin films for optoelectronic applications, Materials Research Bulletin 44 (2009) 1051–1057.
[4] M. Cao, Y. Wang, T. Chen, M. Antonietti, M. Niederberger, A Highly sensitive and fast-responding ethanol sensor based on $CdIn_2O_4$ nanocrystals synthesized by a nonaqueous sol−gel route, Chemistry of Materials 20 (2008) 5781–5786.
[5] A.M.E. Raj, B. Subramanian, V. Senthilkumar, M. Jayachandran, C. Sanjeeviraja, Synthesis and characterization of spray pyrolysed $MgIn_2O_4$ spinel thin films for novel applications, Physica E 40 (2008) 467–473.
[6] P.M. Babu, G.V. Rao, P.S. Reddy, S. Uthanna, Preparation and characterization of polymer metal composite microspheres, Materials Letters 60 (2006) 274–279.
[7] H.M. Ali, H.A. Mohamed, M.M. Wakkad, M.F. Hasaneen, Properties of transparent conducting oxides formed from CdO alloyed with In_2O_3, Thin Solid Films 515 (2007) 3024–3029.
[8] J.H. Lee, H.J. Park, K. Yoo, B.W. Kim, J.C. Lee, S. Park, Characteristics of nano-sized $ZnGa_2O_4$ phosphor prepared by solution combustion method and solid state reaction method, Journal of the European Ceramic Society 27 (2007) 965–968.
[9] T. Omata, N. Ueda, N. Hikuma, K. Ueda, H. Mizoguchi, T. Hashimoto, H. Kawazoe, New oxide phase with wide band gap and high electroconductivity $CdGa_2O_4$ spinel, Applied Physics Letters 62 (1993) 499–506.
[10] T. Moriga, D.D. Edwards, T.O. Mason, G.B. Palmer, K.R. Poeppelmeier, J.L. Schindler, C.R. Kannewurf, I. Nakabayashi, Phase relationships and physical properties of homologous compounds in the Zinc oxide–Indium oxide system, Journal of the American Ceramic Society 81 (1998) 1310–1316.
[11] C. Yaicle, A. Blacklocks, A.V. Chadwick, J. Perriere, A. Rougier, Relationship between structure and deposition conditions for $CuInO_2$ thin films, Applied Surface Science 254 (2007) 1343–1346.
[12] Y. Wang, T. Chen, Q. Mu, G. Wang, A nonaqueous sol–gel route to synthesize $CdIn_2O_4$ nanoparticles for the improvement of formaldehyde-sensing performance, Scripta Materialia 61 (2009) 935–938.
[13] C. Xiangfeng, High sensitivity chlorine gas sensors using $CdIn_2O_4$ thick film prepared by co-precipitation method, Materials Research Bulletin 38 (2003) 1705–1711.
[14] J. Yu, B. Huang, Y. Dai, X. Qin, X. Zhang, Z. Wang, S. Wang, High gas sensitivity of pure $CdIn_2O_4$ hollow spheres for hydrocarbons, Solid State Science 13 (2011) 1315–1319.
[15] G.N. Chandhari, M. Avi, H.G. Wankhade, A.B. Bodade, S.V. Manorama, Nanocrystalline chemically modified $CdIn_2O_4$ thick films for H_2S gas sensor, Thin Solid Films 520 (2012) 4057–4062.
[16] C.W. Teplin, T. Kaydanova, D.L. Young, J.D. Perkins, D.S. Ginley, A. Ode, D.W. Readey, A simple method for the preparation of transparent p-type Ca-doped $CuInO_2$ films: pulsed-laser deposition from air-sintered Ca-doped $Cu_2In_2O_5$ targets, Applied Physics Letters 85 (2004) 3789 (3 pages).
[17] M. Bosacka, E. Filipek, P. Sulcova, Z. Dohnalova, A. Paczesna, Phase equilibria in the solid state and colour properties of the CuO–In_2O_3 system, Journal of Thermal Analysis and Calorimetry 109 (2012) 605–610.
[18] C.Y. Su, C.Y. Chiu, C.H. Chang, J.M. Ting, Synthesis of $Cu_2In_2O_5$ and $CuInGaO_4$ nanoparticles, Thin Solid Films 531 (2013) 42–48.
[19] M. Niederberger, N. Pinna, J. Polleux, M. Antonietti, A general soft-chemistry route to perovskites and related materials: synthesis of $BaTiO_3$, $BaZrO_3$, and $LiNbO_3$ nanoparticles, Angewandte Chemie International Edition 43 (2004) 2270–2273.
[20] G. Gavnweitner, M. Niederberger, Nonaqueous and surfactant-free synthesis routes to metal oxide nanoparticles, Journal of the American Ceramic Society 89 (2006) 1801–1808.
[21] J. Yu, B. Huang, Z. Wang, X. Qin, X. Zhang, P. Wang, Self-template synthesis of $CdIn_2O_4$ hollow spheres and effects of Cd/In molar ratios on its morphologies, Inorganic Chemistry 48 (2009) 10548–10552.
[22] D. Gingasu, I. Mindru, G. Marinescu, L. Patron, C. Ghica, Ultrafine particles of $ZnGa_2O_4$ obtained by solution combustion and complexation methods, Journal of Alloys and Compounds 481 (2009) 890–895.
[23] R.C. Mehrota, R. Bohra, Metal Carboxylates, Acad. Pres, London, 1983.
[24] D.G. Tuck, in: G. Wilkinson, F.G.A. Stone, E.W. Abel (Eds.), Comprehensive Organometallic Chemistry, vol. 1, Pergamon Press, NY, 1982.
[25] B. Gomez-Lor, E. Gutierez-Puebla, M. Iglesias, M.A. Monge, C. Ruiz-Valero, N. Snejko, Novel 2D and 3D Indium metal-organic frameworks: topology and catalytic properties, Chemistry of Materials 17 (2005) 2568–2573.
[26] Z.Z. Lin, L. Cheng, F. Jiang, M. Hong, The indium–carboxylate chain structure with the rectangular tunnels, Inorganic Chemistry Communications 8 (2005) 199–201.
[27] E.V. Anokhina, M. Vougo-Zanda, X. Wang, A.J. Jacobson, In(OH) BDC · 0.75BDCH2 (BDC = Benzenedicarboxylate), a hybrid inorganic−organic vernier structure, Journal of the American Chemical Society 127 (2005) 15000–15001.
[28] Z.Z. Lin, F. Jiang, L. Chen, D. Yuan, M. Hong, New 3-D chiral framework of Indium with 1,3,5-benzenetricarboxylate, Inorganic Chemistry 44 (2005) 73–76.
[29] C. Volkringer, T. Loiseau, A new indium metal-organic 3D framework with 1,3,5-benzene-tricarboxylate, MIL-96 (In), containing μ_3-oxo-centered trinuclear units and a hexagonal 18-ring network, Materials Research Bulletin 41 (2006) 948–954.
[30] M. Vougo-Zanda, X. Wang, A.J. Jacobson, Influence of ligand geometry on the formation of In−O chains in metal–oxide organic frameworks (MOOFs), Inorganic Chemistry 46 (2007) 8819–8824.
[31] R.C. Bott, G. Smith, D.S. Sagatys, D.E. Lynck, C.H.L. Kennard, Group 15 complexes with α-hydroxy carboxylic acids: 7. The preparation and structure determination of sodium (+)-tartrato arsenate(III), $[Na_8As_{10}(C_4H_2O_6)_8(C_4H_3O_6)_2(H_2O)_{19}]_n$; Silver(I) (+)-Tartrato Arsenate(III), $[Ag_9As_{10}(C_4H_2O_6)_9(C_4H_3O_6)(H_4As_2O_5)\ (H_2O)_{10}]_n$ and Rubidium Citrato Antimonate(III), $[Rb_2Sb_4(C_6H_5O_7)_2(C_6H_6O_7)_2(C_6H_7O_7)_4(H_2O)_2]$, Australian Journal of Chemistry 53 (2000) 917–920.
[32] R.L. Schmidt, J. Felsche, Thermal decomposition of Cu(II)(C4H4O6) 3H2O and Co(II)(C4H4O6) 2.5H2O. determination of mechanism by means of simultaneous thermal analysis and mass spectrometry, Thermochimica Acta 59 (1982) 105–114.
[33] S.K. Arora, A. Kothari, B. Amin, B. Chudasama, Synthesis and characterization of cadmium tartrate single crystals, Crystal Research and Technology 42 (2007) 589–594.
[34] A.S.F. Au-Yeung, H.H.Y. Sung, J.A.K. Cha, A.W.-H. Siu, S.S.-Y. Chui, I.D. Williams, Hydrothermal synthesis of indium tartrates: structures of the chiral polymer $[In(L\text{-}TAR)^{3-}H_2O]\cdot 0.5H_2O$ containing the tartrate trianion, and a microporous hybrid solid $[In(OH)(D/L\text{-}TAR)^{2-}]\cdot 2H_2O$, Inorganic Chemistry Communications 9 (2006) 507–511.
[35] F. Jian, P. Zhao, Q. Wang, Synthesis and crystal structure of a novel tartrate copper(II) two-dimensional coordination polymer: $\{[Cu_2(C_4H_4O_6)_2(H_2O)_2]\cdot 4H_2O\}$, Journal of Coordination Chemistry 58 (2005) 1133–1138.
[36] I. Mindru, G. Marinescu, D. Gingasu, L. Patron, L. Diamandescu, C. Ghica, B. Mironov, Doped aluminium based spinels synthesized by a soft chemistry method, Materials Science and Engineering: B 170 (2010) 99–106.
[37] I. Mindru, G. Marinescu, D. Gingasu, L. Patron, C. Ghica, M. Giurginca, Blue $CoAl_2O_4$ spinel *via* complexation method, Materials Chemistry and Physics 122 (2010) 491–497.
[38] D. Gingasu, I. Mindru, L. Patron, S. Stoleriu, Synthesis of lithium ferrites from polymetallic carboxylates, Journal of the Serbian Chemical Society 73 (2008) 979–988.
[39] C. Suciu, I. Mindru, G. Marinescu, O. Carp, L. Patron, $LnAlO_3$ obtained by the complexation and the self-propagating combustion methods, Journal of Optoelectronics and Advanced Materials 10 (2008) 1452–1456.
[40] N.B. Colthup, L.H. Daly, S.E. Wiberley, in: Introduction to infrared and Raman spectroscopy, Academic Press, New York, 1975.
[41] (a) A.B.P. Lever, Inorganic Electronic Spectroscopy, Amsterdam-London-New York, Elsevier Publishing Company, 1968;
(b) P. Mukherjee, M.G.B. Drew, A. Ghosh, Anion-directed template synthesis and hydrolysis of Mono-Condensed Schiff base of 1,3-pentanediamine and o-Hydroxyacetophenone in Ni^{II} and Cu^{II} complexes, European Journal of Inorganic Chemistry 21 (2008) 3372–3381.

[42] Z. Zou, J. Ye, K. Oka, Y. Nishihara, Synthesis and properties of $In_{2-x}Zn_xCu_2O_5$ ($x=0$, 1) compounds, Journal of Materials Science Letters 17 (1998) 1191–1193.

[43] H.R. Freund, H.k. Müeller-Baschbaum, Üer Oxocuprate. XXV Zur Kenntnis von In2Cu2O5, Zeitschrift fuer *Anorganische und Allgemeine Chemie* 441, (1978) 103–106.

[44] G. Bergerhoff, H. Kasper, Die Kristallstruktur des Kupfer-Indium-Oxids, $Cu_2In_2O_5$, Acta Crystallographica B 24 (1968) 388–391.

[45] O. Schmitz-DuMont, H. Kasper, Farbe und Konstitution bei anorganischen Feststoffen, 10. Mitt.: Die Lichtabsorption des zweiwertigen Kupfers im Kupferindiumoxid und analogen Verbindungen mit Yttrium und einigen Lanthaniden, Monatshefte fuer Chemie 96 (1965) 506–515.

[46] M.N. Popova, S.A. Klimin, R. Troc, Z. Bukowski, Magnetic phase transitions and magnetic structures of $In_2Cu_2O_5$ and $Sc_2Cu_2O_5$, Solid State Communications 102 (1997) 71–75.